Low-energy Electron Reflectivity from Graphene

R. M. Feenstra, N. Srivastava, Qin Gao, and M. Widom
Dept. Physics, Carnegie Mellon University, Pittsburgh, Pennsylvania 15213

Bogdan Diaconescu, Taisuke Ohta, and G. L. Kellogg
Sandia National Laboratories, Albuquerque, New Mexico 87185

J. T. Robinson
Naval Research Laboratory, Washington, D.C. 20375

I. V. Vlassiouk
Oak Ridge National Laboratory, P.O. Box 2008, Oak Ridge, Tennessee 37831

Supplemental Material

Theoretical Method

Computations are performed in a periodically repeated vacuum-graphene-vacuum system, with at least 1 nm vacuum separating the graphene slabs. Assuming an incoming electron beam at normal incidence, we need only consider states in the graphene having wavevector $\mathbf{k}$ with components $k_x = k_y = 0$ and $k_z \neq 0$ (with z labeling the direction perpendicular to the graphene planes and $z = 0$ being the center of the graphene slab). Two wavefunctions with energy E_{ν,k_z} are obtained, $\psi_{\nu,k_z}(x,y,z)$ and $\psi_{\nu,-k_z}(x,y,z)$, where ν is a band index. We work in terms of Fourier components of the wavefunction with reciprocal lattice $\mathbf{G} \equiv (G_x, G_y, G_z)$,

$$\psi_{\nu,\mathbf{k}}(\mathbf{r}) = \sum_{\mathbf{G}} \frac{C_{\nu,\mathbf{G}}}{\sqrt{V}} e^{i(\mathbf{k}+\mathbf{G})\cdot\mathbf{r}} = \sum_{G_x,G_y} \phi_{\nu,k_z}^{G_x,G_y}(z)\, e^{i[(k_x+G_x)x+(k_y+G_y)y]} \tag{1}$$

where $C_{\nu,\mathbf{G}}$ is a plane-wave expansion coefficient (obtained from the electronic structure computation), V is the volume of a unit cell (included for normalization purposes), and with

$$\phi_{\nu,k_z}^{G_x,G_y}(z) = \sum_{G_z} \frac{C_{\nu,\mathbf{G}}}{\sqrt{V}} e^{i(k_z+G_z)z}. \tag{2}$$

Our evaluations are performed for $\mathbf{k} = (0,0,k_z)$, so we need only consider $\psi_{\nu,k_z}(\mathbf{r})$ in comparison to $\phi_{\nu,k_z}^{G_x,G_y}(z)$. Far out in the vacuum, the wavefunctions $\psi_{\nu,k_z}(\mathbf{r})$ have a specific, separable form: they consist of travelling waves $\exp(i\kappa_{\mathbf{g}} z)$ where $\kappa_{\mathbf{g}}$ labels the z-component of the wavevector in the vacuum, multiplied by a sum of lateral waves of the form

$A_{\mathbf{g}} \exp[i(g_x x + g_y y)]$ where the lateral wavevector is denoted by $\mathbf{g} = (g_x, g_y)$ and $A_{\mathbf{g}}$ is an amplitude. We have $\kappa_{\mathbf{g}} = \sqrt{2m(E_{\nu,k} - E_V)/\hbar^2 - g_x^2 - g_y^2}$ where E_V is the vacuum energy (corresponding to the potential energy at a *z*-value sufficiently far from the graphene slab so that the potential is essentially constant; we find that a distance of about 0.5 nm is sufficient for this purpose). The lateral wavevector will correspond to one of the (G_x, G_y) values; $(g_x, g_y) = (0,0)$ for the nondiffracted beam and $(g_x, g_y) \neq (0,0)$ for a diffracted beam, the latter existing only for $E_{\nu,k} - E_V \geq \hbar^2(g_x^2 + g_y^2)/2m$. Of course, evanescent states will exist for lower energies, but we are considering distances far enough out in the vacuum so that we do not need to consider those. We note that the values of $\kappa_{\mathbf{g}}$ are quite different than those of k_z. For electron energies of 0 – 10 eV the former range over $0 < \kappa_{\mathbf{g}} < 16$ nm^{-1} with $(g_x, g_y) = (0,0)$. The latter are determined by the simulation size in the *z*-direction; with $-z_S < z \leq z_S$ we have $-\pi/2z_S < k_z \leq \pi/2z_S$, which for a typical value $2z_S \approx 5$ nm gives $|k_z| < 0.63$ nm^{-1}.

Thus, far out in the vacuum, each eigenstate will consist of a possibly nonzero $\phi_{\nu,k_z}^{0,0}(z)$ component, together with some number of nonzero $\phi_{\nu,k_z}^{G_x,G_y}(z)$ components (one for single diffraction or a few for multiple diffraction, along with equivalent components obtained by symmetry operations), where again, the maximum value of (G_x, G_y) is determined by $2m(E_{\nu,k} - E_V)/\hbar^2 \geq G_x^2 + G_y^2$. In the following discussion we will assume energies low enough so that no diffracted beams occur, which for graphene corresponds to $E < 33.0$ eV with a primitive hexagonal lattice constant of $a = 0.2464$ nm. In this case, any wavefunction that has a significant amplitude far out in the vacuum corresponds to a (0,0) nondiffracted beam. The precise criterion we use to distinguish between a (0,0) beam and other states will be specified shortly. Give this discrimination, we then proceed with the analysis needed to compute the reflectivity.

From the electronic structure computation we obtain $\phi_{\nu,k_z}^{0,0}(z)$, employing Eq. (2). For our analysis we also require $\phi_{\nu,-k_z}^{0,0}(z)$, which for the case of a potential that has a mirror plane at $z = 0$ can be easily obtained from $\phi_{\nu,-k_z}^{0,0}(z) = \phi_{\nu,k_z}^{0,0}(-z)$. For a nonsymmetric potential we must use Eq. (2) to obtain $\phi_{\nu,-k_z}^{0,0}(z)$, but in this case we also must ensure that a definite phase relationship exists between $\phi_{\nu,k_z}^{0,0}(z)$ and $\phi_{\nu,-k_z}^{0,0}(z)$ (i.e. between ψ_{ν,k_z} and $\psi_{\nu,-k_z}$). This is achieved by taking the phase of $\phi_{\nu,k_z}^{0,0}(z)$ to be zero at $z = -z_S$ and the phase of $\phi_{\nu,-k_z}^{0,0}(z)$ to be zero at $z = +z_S$. We then form the linear combinations

$$\phi_{\nu,+}^{0,0}(z) = [\phi_{\nu,k_z}^{0,0}(z) + \phi_{\nu,-k_z}^{0,0}(z)]/\sqrt{2} \qquad 3(a)$$

$$\phi_{\nu,-}^{0,0}(z) = [\phi_{\nu,k_z}^{0,0}(z) - \phi_{\nu,-k_z}^{0,0}(z)]/\sqrt{2} \ . \qquad 3(b)$$

In addition to having a nonzero value for k_z, we also perform the evaluations only for k_z not at the edge of the Brillouin zone (i.e. of the simulation cell), thus ensuring that both $\phi_{\nu,+}^{0,0}$ and $\phi_{\nu,-}^{0,0}$ are nonzero.

The functions $\phi_{\nu,+}^{0,0}$ and $\phi_{\nu,-}^{0,0}$ form standing-wave type states, i.e. any complex phase that they might have is a constant, independent of z [similarly for the linear combinations of the full states $\psi_{\nu,+} = (\psi_{\nu,k_z} + \psi_{\nu,-k_z})/\sqrt{2}$ and $\psi_{\nu,-} = (\psi_{\nu,k_z} - \psi_{\nu,-k_z})/\sqrt{2}$]. For a symmetric potential these two functions are even and odd, respectively, although our analysis method works even for asymmetric potentials. Now, consider a range of z-values sufficiently far from the graphene slab so that the potential is essentially constant (and equal to the vacuum level); let us label these vacuum regions of $-z_S \le z \le -z_L$ on the left-hand side of the slab and $z_R \le z \le z_S$ on the right. In these vacuum regions, the standing waves defined by Eqs. (3a) and (3b) can be expressed simply as cosine or sine functions, with some respective phase shifts δ_+, δ'_+, δ_-, and δ'_-, according to

$$\phi_{\nu,+}^{0,0}(z) = \begin{cases} A_+ \cos(\kappa_0 z + \delta_+), & -z_S \le z \le -z_L \qquad (4a) \\ A_+ \cos(\kappa_0 z - \delta'_+), & z_R \le z \le z_S \qquad (4b) \end{cases}$$

$$\phi_{\nu,-}^{0,0}(z) = \begin{cases} A_- \sin(\kappa_0 z + \delta_-), & -z_S \le z \le -z_L \qquad (4c) \\ A_- \sin(\kappa_0 z - \delta'_-) & z_R \le z \le z_S \qquad (4d) \end{cases}$$

where $\kappa_0 \equiv \kappa_{0,0} = \sqrt{2m(E - E_V)}/\hbar$ is the free-electron wavevector. For a symmetric potential we have, of course, $\delta_+ = \delta'_+$ and $\delta_- = \delta'_-$. The phase shifts are determined by searching over the range $-z_S \le z \le -z_L$ and $z_R \le z \le z_S$ for zeroes of $\phi_{\nu,-}^{0,0}$ and zeroes in the derivative of $\phi_{\nu,+}^{0,0}$.

To obtain the reflectivity, we form appropriate linear combinations of $\phi_{\nu,+}^{0,0}$ and $\phi_{\nu,-}^{0,0}$ corresponding to only a transmitted wave (traveling in the $+z$ direction) for $z_R \le z \le z_S$ and with both incident and reflected waves (traveling in the $+z$ and $-z$ directions, respectively) for $-z_S \le z \le -z_L$.[1] To achieve this, we first form the two combinations $\phi_{\nu,+}^{0,0} \pm i\phi_{\nu,-}^{0,0}$, which equal $A_+ \cos(\kappa_0 z - \delta'_+) \pm iA_- \sin(\kappa_0 z - \delta'_-)$ far on the right-hand side. We then separate these into their $\exp(+i\kappa_0 z)$ and $\exp(-i\kappa_0 z)$ components and form a further linear combination $A_1(\phi_{\nu,+}^{0,0} + i\phi_{\nu,-}^{0,0}) + A_2(\phi_{\nu,+}^{0,0} - i\phi_{\nu,-}^{0,0})$ such that the prefactor of the $\exp(-i\kappa_0 z)$ term is zero. This is achieved by taking $A_1 = (A_+ e^{i\delta'_+} + A_- e^{i\delta'_-})/2$ and $A_2 = -(A_+ e^{i\delta'_+} - A_- e^{i\delta'_-})/2$. Forming

the same set of linear combinations on the far left-hand side yields a reflectivity (ratio of reflected to incident electron current) of

$$R = \left| \frac{e^{i(\delta'_+ - \delta_-)} - e^{-i(\delta_+ - \delta'_-)}}{e^{i(\delta'_+ + \delta_-)} + e^{i(\delta_+ + \delta'_-)}} \right|^2 \tag{5a}$$

and a transmission of

$$T = \left| \frac{2\cos(\delta'_+ - \delta'_-)}{e^{i(\delta'_+ + \delta_-)} + e^{i(\delta_+ + \delta'_-)}} \right|^2 . \tag{5b}$$

For a symmetric potential these formulas simplify to $R = \sin^2(\delta_+ - \delta_-)$ and $T = \cos^2(\delta_+ - \delta_-)$ so that, obviously, $R + T = 1$. From the forms of Eqs. (5a) and (5b) it is not so obvious that $R + T = 1$ for the general case, but we find that this relationship is always satisfied so long as the phase normalization mentioned preceding Eqs. (3a) and (3b) is performed.

The above analysis method is illustrated in Fig. S1. Figure S1(a) shows $\phi^{0,0}_{\nu,k_z}(z)$ for a typical electronic state (this state is the same one discussed in Figs. 1 – 3 of Ref. [2]), and the corresponding $\phi^{0,0}_{\nu,-k_z}(z)$ is pictured in Fig. S1(b). Figures S1(c) and S1(d), respectively, show the resultant $\phi^{0,0}_{\nu,+}$ and $\phi^{0,0}_{\nu,-}$. Figures S1(e) and S1(f) show the linear combinations $\phi_1 \equiv \tilde{\phi}^{0,0}_{\nu,+} + i\tilde{\phi}^{0,0}_{\nu,-}$ and $\phi_2 \equiv \tilde{\phi}^{0,0}_{\nu,+} \pm i\tilde{\phi}^{0,0}_{\nu,-}$, respectively, with $\tilde{\phi}^{0,0}_{\nu,\pm}$ being equal to $\phi^{0,0}_{\nu,\pm}$ multiplied by a phase factor such that the product is purely real. Finally, Fig. S1(g) shows the linear combination $A_1\phi_1 + A_2\phi_2$, where it clear that only an outgoing state is formed on the right-hand side of the slab since the magnitude of the wavefunction is seen to be constant there. Note that this wavefunction at $+z_S$ differs from that at $-z_S$, which is a consequence of that fact that $\phi^{0,0}_{\nu,k_z}(z)$ contains a part that is not periodic over the simulation interval $-z_S < z \le z_S$ [i.e. a $\exp(ik_z z)$ term].

Returning to the procedure used to test if $\phi^{0,0}_{\nu,+}$ and $\phi^{0,0}_{\nu,-}$ have significant amplitude, we integrate these functions over $-z_S \le z \le -z_L$ forming

$$\sigma_\pm \equiv \frac{\sqrt{A z_S}}{z_S - z_L} \int_{-z_S}^{-z_L} \phi^{0,0}_{\nu,\pm}(z) \exp(i\kappa_0 z) \quad \text{and} \tag{6a}$$

$$\sigma \equiv \left[\left|\sigma_+\right|^2 + \left|\sigma_-\right|^2 \right]^{1/2} \tag{6b}$$

where A is the area of the unit cell in the (x,y) plane. The $\exp(i\kappa_0 z)$ term occurs in the integrand here since we are considering the inner product of $\phi^{0,0}_{\nu,+}$ and $\phi^{0,0}_{\nu,-}$ with a plane wave propagating in the $+z$ direction. The values for σ thus obtained have magnitude near unity for the propagating (0,0) states of interest and are negligible ($\lesssim 10^{-6}$, due to numerical resolution of the computation) for most other states. We can thus set a discriminator for the σ-values of, say, 10^{-3}, to include only the states with substantial $\phi^{0,0}_{\nu,k}(z)$ amplitude.

An exception to this sorting of the states is found to occur, when, in certain cases, a state of "mixed" (g_x, g_y) character forms, e.g. a mixed (0,0), (1,0), and $(0,-1)$ state. Such states contain $\phi^{1,0}_{\nu,k_z}(z)$ and $\phi^{-1,0}_{\nu,k_z}(z)$ terms that dominate the wavefunction within the graphene slab, but they also contains a small, nonzero $\phi^{0,0}_{\nu,k_z}(z)$ term that constitutes the only contribution to the wavefunction far out in the vacuum. Such states appear to be precursors to diffracted states, i.e. at higher energy the $\phi^{1,0}_{\nu,k_z}(z)$ and $\phi^{-1,0}_{\nu,k_z}(z)$ terms would have nonzero amplitude in that vacuum and they could be combined to form diffracted beams. For these mixed states, the measure of σ produces values intermediate between 10^{-6} and 1, with values in the 10^{-2} or 10^{-1} range specifically found to occur. Again, it is necessary to reject these mixed states from the analysis, and for this reason we typically use a discriminator for the σ-values that is close to 1; a value of 0.8 is used for all results reported in this work and this value works for the present computations to reject all mixed states.

Even though our analysis method for the (0,0) beam relies on the use $\phi^{0,0}_{\nu,k}(z)$, i.e. the (0,0) Fourier component of the wavefunction, it should be emphasized that the method does indeed fully include all multiple scattering within the slab. The electronic structure solutions do, of course, contain all of that multiple scattering, and we fully employ those solutions in our analysis. Our use of the (0,0) Fourier component is made, in essence, in order to match the full wavefunction to a plane wave far out in the vacuum.

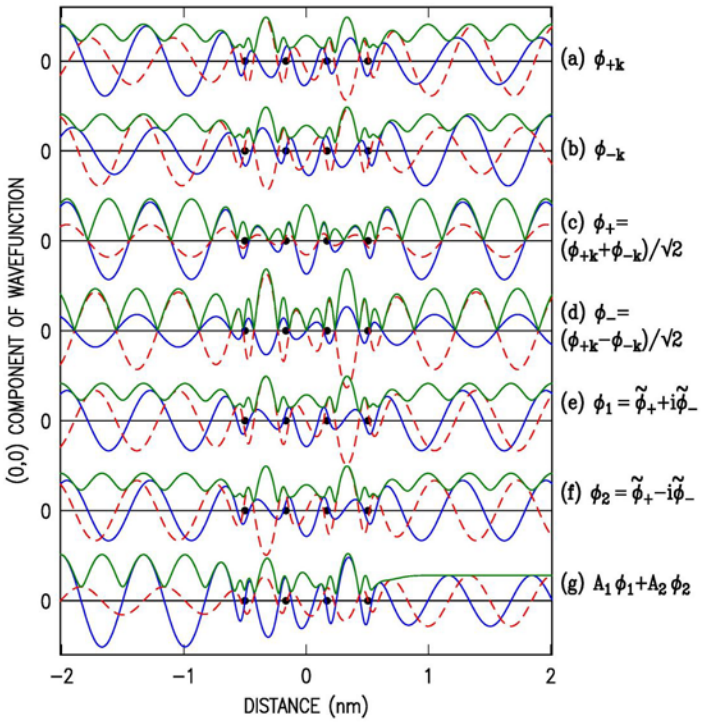

FIG S1. Wavefunctions for various states of 4-layer graphene, plotted over the entire simulation interval $-z_S < z \le z_S$ and illustrating the process used to deduce the reflectivity: (a) a typical state, having wavevector $k_z = 0.39\ \mathrm{nm}^{-1}$ and energy 3.24 eV above the vacuum level, (b) the corresponding state with negative wavevector, (c) and (d) linear combinations of these two $+k_z$ and $-k_z$ states. (e) and (f) Further linear combinations, which ultimately yield the state shown in (g) that has only an outgoing plane wave on the right-hand side of the graphene slab (see text). The real-part of the wavefunctions are shown by a solid blue line and the imaginary parts by a dashed red line, with the magnitude shown by a solid green line.

References

---

[1] The reader is reminded that $\phi^{0,0}_{\nu,+}$ and $\phi^{0,0}_{\nu,-}$ are equal to $\psi_{\nu,+} = (\psi_{\nu,k} + \psi_{\nu,-k})/\sqrt{2}$ and $\psi_{\nu,-} = (\psi_{\nu,k} - \psi_{\nu,-k})/\sqrt{2}$, respectively, far out in the vacuum, so this linear combination procedure yields the appropriate *full wavefunctions* of the incident, transmitted and reflected waves. Actually, the entire analysis procedure can be performed using $\psi_{\nu,+}(x,y,z)$ and $\psi_{\nu,-}(x,y,z)$ rather than $\phi_{\nu,+}(z)$ and $\phi_{\nu,-}(z)$. The only difference is that, in the former case, a slight dependence might exist in the results on the *x* and *y* locations used for the evaluations, i.e. if the distance out into the vacuum is insufficiently large. This dependence is entirely absent when using $\phi_{\nu,+}(z)$ and $\phi_{\nu,-}(z)$.

[2] R. M. Feenstra and M. Widom, arXiv:1212.5506 [cond-mat.mes-hall] (2012), submitted to Ultramicroscopy.